Off-center rattling modes and glasslike thermal conductivity in the type-I clathrate $Ba_8Ga_{16}Sn_{30}$

K. Suekuni,[1] Y. Takasu,[2] T. Hasegawa,[3] N. Ogita,[3] M. Udagawa,[3,4] M. A. Avila,[1,*] and T. Takabatake[1,4]
[1]*Department of Quantum Matter, ADSM, Hiroshima University, Higashi-Hiroshima 739-8530, Japan*
[2]*St. Marianna University School of Medicine, Kawasaki, Kanagawa 216-8511, Japan*
[3]*Graduate School of Integrated Arts and Sciences, Hiroshima University, Higashi-Hiroshima 739-8521, Japan*
[4]*Institute for Advanced Materials Research, Hiroshima University, Higashi-Hiroshima 739-8530, Japan*
(Received 29 November 2009; revised manuscript received 24 February 2010; published 19 May 2010)

Type-I clathrate $Ba_8Ga_{16}Sn_{30}$ is unique for showing glasslike behavior in the lattice thermal conductivity κ_L irrespective of the charge carrier type. For better understanding the relation between this behavior and guest rattling, polarized Raman-scattering measurements have been performed on carrier-tuned single crystals. The appearance of a symmetry-forbidden mode in the E_g symmetry spectrum indicates that the Ba atoms are rotating among the off-center positions in the tetrakaidecahedron. On cooling from 300 to 4 K, the energies of E_g and T_{2g} guest modes decrease by 15% and 25%, respectively. This drastic decrease originates from the strongly anharmonic potential with a quartic term of the atomic displacement. The energy of 14 cm^{-1} for the T_{2g} mode at 4 K is the lowest among intermetallic clathrates. These results for $Ba_8Ga_{16}Sn_{30}$ are compared with those for type-I $Eu_8Ga_{16}Ge_{30}$ and $Sr_8Ga_{16}Ge_{30}$ whose $\kappa_L(T)$ show similar glasslike behavior with a plateau. The comparison between three systems indicates that the guest rattling energy is proportional to the temperature range of the plateau in $\kappa_L(T)$.

DOI: 10.1103/PhysRevB.81.205207 PACS number(s): 82.75.−z, 63.20.Ry, 65.40.−b, 78.30.−j

I. INTRODUCTION

Anharmonic vibrations of guest atoms encapsulated in an oversize cage are referred to as "rattling" which often occurs in intermetallic clathrates as well as filled skutterudites and β-pyrochlore oxides.[1–3] The rattling is thought to give rise to various interesting phenomena, such as suppression of thermal conductivity in type-I clathrates $Sr_8Ga_{16}Ge_{30}$ (SGG) and β-$Eu_8Ga_{16}Ge_{30}$ (β-EGG),[1,4–8] heavy-fermion behavior in the filled skutterudite $SmOs_4Sb_{12}$,[9] and strong coupling superconductivity in β-pyrochlore KOs_2O_6.[10] Type-I clathrates have a cubic primitive structure which is composed of two kinds of cages, dodecahedron and tetrakaidecahedron. The guest in the tetrakaidecahedron is loosely bound to the cage and therefore vibrates with larger amplitude and lower energy than the cage atoms.

The lattice part of thermal conductivity, $\kappa_L(T)$, for $X_8Ga_{16}Ge_{30}$ with X=Sr and Eu shows glasslike behavior as presented in Fig. 1. The κ_L is approximately proportional to T^2 below 1 K, unlike the typical T^3 dependence in crystalline materials.[7,8] By association with glassy systems, the T^2 behavior has been attributed to phonon scattering by tunneling of two-level systems, whereas the plateau at around 10 K is attributed to resonant phonon scattering by the guest rattling.[1,4,7,8] At room temperature, the magnitude of κ_L for $X_8Ga_{16}Ge_{30}$ (X=Sr and Eu) is in the range 0.6–1.3 W/K m,[1] being lower than that of the vitreous SiO_2 1–2 W/K m.[11] The important role of umklapp process in the acoustic-phonon scattering was pointed out based on inelastic neutron-scattering study of the filled skutterudite.[12] An umklapp process can occur even for low-energy acoustic phonons by means of weakly dispersive rattling phonons with a low-energy level of approximately 50 K. This idea has been applied to explain the low value of κ_L in the clathrate $Ba_8Ga_{16}Ge_{30}$ (BGG).[13]

Raman-scattering spectroscopy has been proved to be a powerful method to investigate dynamical properties of guest rattling in various clathrates,[14–16] in spite of the fact that not all vibrational modes can be detected by this technique. In type-I clathrates, the vibrational modes of the guests in the dodecahedron ($X1$) are Raman inactive, while those in the tetrakaidecahedron ($X2$) are Raman active. Taking advantage of this site selection, we have determined the symmetry and energy of the rattling for $X2$ in $X_8Ga_{16}Ge_{30}$ (X=Eu, Sr, and Ba) and $X_8Ga_{16}Si_{30-x}Ge_x$ (X=Sr and Ba).[15,16] In β-EGG and SGG the Eu2 and Sr2 rattling modes are described as a rotation mode among the off-center sites. On the other hand, for BGG the Ba2 mode is described as nearly on-center vibration. The energies for $X2$=Ba, Sr, and Eu in $X_8Ga_{16}Ge_{30}$ are 46 K, 42 K, and 26 K, respectively, at 2 K.[15] This energy sequence is in agreement with those derived from inelastic neutron scattering and nuclear inelastic scattering.[17] Furthermore, this sequence directly correlates with the lowering of κ_L. Thus, the rattling is thought to give rise to the glasslike behavior of $\kappa_L(T)$ in the systems with $X2$=Eu and Sr.

Recently, single-crystal x-ray diffraction studies of type-I $Ba_8Ga_{16}Sn_{30}$ (β-BGS) revealed that the Ba2 guests have large off-center displacements of 0.4 Å irrespective of the charge carrier type.[18] Both n- and p-type crystals show glasslike behavior in $\kappa_L(T)$ as is shown in Fig. 1. Analysis of the specific heat has given a characteristic energy of 20 K for the Ba2 rattling, which is lower than 26 K for Eu2 in β-EGG.[15,16,18,19] In this work, we have performed Raman-scattering experiments in the temperature range from 4 to 300 K to investigate the symmetry and energy of Ba2 rattling in *off-center* and *glassy* system β-BGS in detail. The preliminary analysis of the spectra at 5 K has been reported in a previous paper.[20] We demonstrate here a correlation between the guest rattling energy and the temperature range of the plateau in $\kappa_L(T)$ by comparing the data with those for β-EGG and SGG.[15,16]

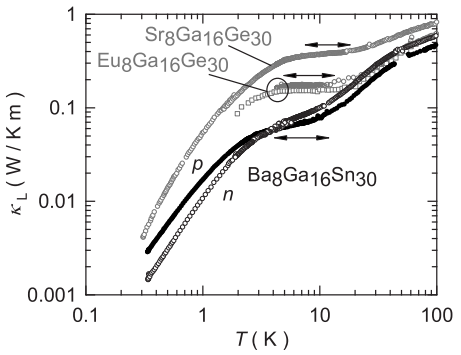

FIG. 1. Temperature dependence of lattice thermal conductivity κ_L for n- and p-type β-$Ba_8Ga_{16}Sn_{30}$, β-$Eu_8Ga_{16}Ge_{30}$ [open circles; our data, open squares; Bentien *et al.* (Ref. 5)], and $Sr_8Ga_{16}Ge_{30}$ (Ref. 8). The arrows show the temperature ranges of the plateaus.

II. EXPERIMENTAL

Single crystals of β-BGS were grown by a self-flux method, which was detailed in previous papers.[18,19] The carrier types were controlled by adjusting the Ga/Sn ratio in the initial flux from which the crystals precipitate. High-purity elements of Ba, Ga, and Sn were mixed in an argon-filled glovebox and sealed in a quartz ampoule, in proportions of 8:16:50 for the n-type samples and 8:32:60 for p-type ones. The ampoules were soaked at 900 °C for 4 h, cooled to 600 °C in 1 h, and then slowly cooled to 400 °C over 100 h. Polyhedral single crystals of about 5 mm in diameter were obtained. The actual elemental composition of the grown crystals was determined by a wavelength dispersive electron-probe microanalyzer. It was found that all crystals have excess Sn by 0.1–0.2 with respect to the ideal composition 30.[19] At room temperature, the values of electrical resistivity are in the range 20–40 mΩ cm for both n and p type, and the thermopower is −300 μV/K for n type and 250 μV/K for p type. The carrier concentrations of both type samples have been estimated to be approximately $10^{19}/cm^3$ from Hall effect measurements.[19]

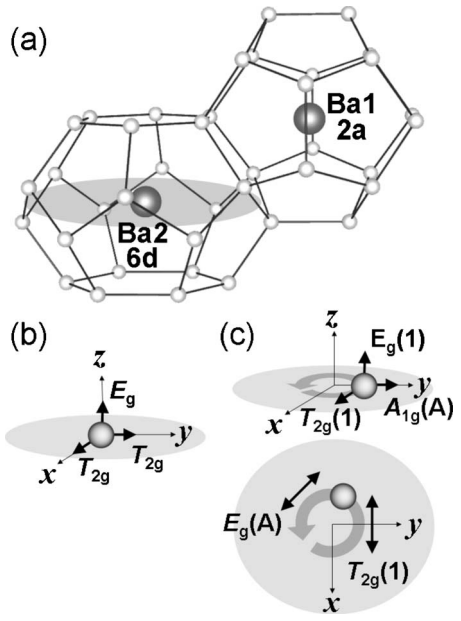

FIG. 2. (a) The dodecahedral and tetrakaidecahedral cages of the type-I clathrate structure. The center of the former is a 2a (Ba1) site and that of the latter is a 6d (Ba2) site. (b) On-center vibrational modes of Ba2 with one E_g mode and doubly degenerate T_{2g} modes. (c) Off-center rotational modes of Ba2 with E_g, T_{2g}, and A_{1g} modes. The modes marked by (A) are additional modes which are allowed only for off-center vibrations.

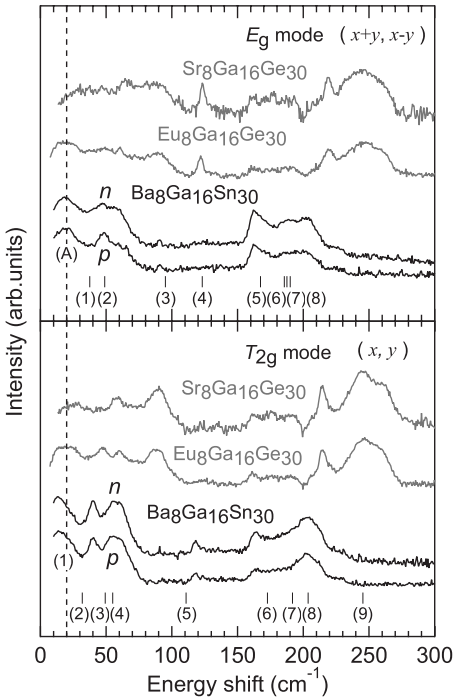

FIG. 3. Raman-scattering spectra of E_g and T_{2g} modes for n- and p-type β-$Ba_8Ga_{16}Sn_{30}$ at 4 K. The spectra at 2 K for β-$Eu_8Ga_{16}Ge_{30}$ and $Sr_8Ga_{16}Ge_{30}$ with n-type carriers are taken from Ref. 15. The peaks marked by (A) and (1) are the guest modes, and other peaks (2)–(9) are the cage modes (see text).

Backward scattered light was analyzed by a triple monochromator (JASCO NR-1800) equipped with a liquid-N_2-cooled charge-coupled-device (CCD) detector (Princeton Instruments Inc. LN/CCD-1100PB) in the energy range between 10 and 740 cm^{-1}. For the excitation light, 514.5 nm wavelength Ar-ion laser was used. Its power at the specimen was kept at less than 7 mW to avoid local heating. The measurements were done at various temperatures between 4 and 300 K.

The group theory for lattice vibrations of type-I clathrates with cubic primitive structure $Pm\bar{3}n$ gives the Raman-active modes $3A_{1g}+7E_g+8T_{2g}$ for the cage atoms and E_g+T_{2g} for the Ba2 guest on the assumption that Ba2 occupies the on-center 6d position [Figs. 2(a) and 2(b)]. The Raman-active phonons with each irreducible representation can be distinguished by polarization-dependent measurements. The polarization geometry is given by the notation (i,j), where i and j denote the polarization directions of the incident and scattered light, respectively. For example, phonon modes with A_{1g} and T_{2g} symmetry appear in (x,x) and (x,y) geometries, respectively, where x and y denote [100] and [010]. On the other hand, the phonon mode with E_g symmetry appears in

TABLE I. Phonon energies of β-$Ba_8Ga_{16}Sn_{30}$ in units of cm^{-1}. Observed energies at 4 K and calculated ones are presented in the obs. and calc. columns, respectively. The peaks (A) and (1) are guest modes and the others (2)–(9) are cage modes.

		Peaks (label)									
Symmetry		(A)	(1)	(2)	(3)	(4)	(5)	(6)	(7)	(8)	(9)
E_g	Obs.	19	47	59	91		162	168	188	204	
	Calc.		38	49	95	123	168	186	188	190	
T_{2g}	Obs.		14	40	55	62	118	164	183	204	
	Calc.		28*i*	32	49	55	111	173	192	204	245

both (x,x) and $(x+y,x-y)$ configurations. In this study, we measured the spectra in three geometries; (x,x), (x,y), and $(x+y,x-y)$. We do not present the spectra of the A_{1g} mode since the E_g spectra of $(x+y,x-y)$ geometry could not be successfully subtracted from $A_{1g}+E_g$ spectra of (x,x) geometry.

First-principles calculations of the phonon energy were performed assuming that Ba2 occupies the on-center 6*d* position. Thereby, we used the ABINIT code,[21,22] which is based on *ab initio* pseudopotentials and a plane-wave basis set in the framework of the density-functional formalism. The Troullier-Martins-type pseudopotentials[23] were generated using the FHI98PP code.[24] The ground state and response function were calculated with the local-density approximation parameterized by Perdew and Wang[25] and with the Brillouin-zone sampling of a Monkhorst-Pack[26] $2\times2\times2$ mesh of the special q points. The cutoff kinetic energies were set at 34 Ry, where 1 Ry=13.605 eV. Phonon energies were calculated using the density-functional perturbation theory, whose technical details on the computation of responses to atomic displacements and homogeneous electric fields are described in Refs. 27 and 28. The results does not affect on the assignment of the cage modes, even for the assumption of the center Ba2.

III. RESULTS AND DISCUSSION

The Raman spectra of the $E_g(x+y,x-y)$ and T_{2g} (x,y) modes for *n*- and *p*-type β-BGS at 4 K are presented in Fig. 3, together with the spectra of *n*-type β-EGG and *n*-type SGG.[15] The structures for β-BGS in the energy range for E_g mode between 59 and 204 cm^{-1} and that for T_{2g} mode between 40 and 204 cm^{-1} are assigned to the $(Ga,Sn)_{46}$ framework modes. It should be noted that this energy range is lower by approximately 20% than that of $(Ga,Ge)_{46}$ framework modes. The numbering of the peaks from (1) to (9) is based on the calculations. The phonon energies are listed in Table I for all peaks of E_g and T_{2g} observed at 4 K together with calculated ones. In the calculated peaks, the $E_g(1)$ and the $T_{2g}(1)$ modes are the Ba2 guests modes and others at higher energies are Ga/Sn cage modes. The good correspondence between the calculated and observed energies allows us to identify the numbered modes from (2) to (8) and $E_g(1)$ at 47 cm^{-1} which corresponds to the Ba2 vibration perpendicular to the plane [Fig. 2(a)]. For $T_{2g}(1)$ at 14 cm^{-1}, the calculated energy is imaginary value of $28i$ cm^{-1} as shown in Table I. This result suggests that Ba2 is unstable at the on-center 6*d* site. Similar unstable state was pointed out for $Sr_8Ga_{16}Ge_{30}$.[29] If Ba2 were at the 6*d* site, the T_{2g} modes would be degenerate for the vibrations along the x and y directions [Fig. 2(b)]. However, the degenerate modes split into A_{1g}(A) and $T_{2g}(1)$ modes if Ba2 rotate among off-center sites. In the E_g spectra of Fig. 3, we do find the additional E_g mode marked by (A) at the lowest energy of 19 cm^{-1}. This E_g(A) mode corresponds to the tangential displacement along [110] [Fig. 2(c)].[15,16] The presence of this E_g(A) mode is the experimental evidence that Ba2 rotates among off-center sites.

Temperature dependences of the E_g and T_{2g} spectra are presented in Fig. 4 only for the *n*-type sample because the spectra are similar to that for *p*-type one. A noteworthy feature in Fig. 4 is the different temperature dependences between the cage modes and the guest modes. With decreasing temperature from 300 to 4 K, the energies of cage modes slightly increase, for instance, from 159 to 162 cm^{-1} for $E_g(5)$ as is shown in Fig. 5. Such hardening is a natural

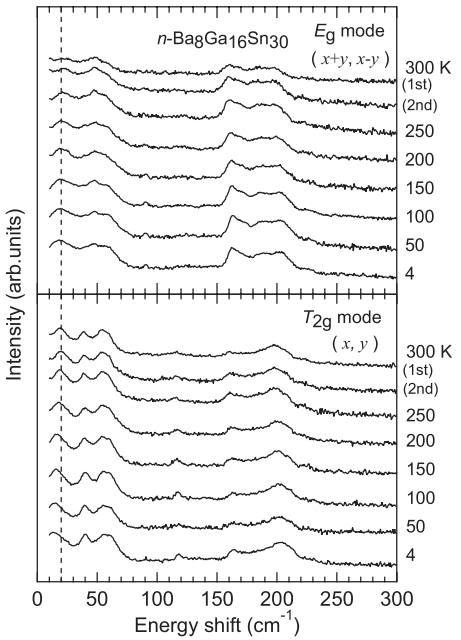

FIG. 4. Raman-scattering spectra of E_g and T_{2g} modes for *n*-type β-$Ba_8Ga_{16}Sn_{30}$ at various temperatures from 4 to 300 K. The spectra at 300 K are reproducible before (1st) and after cooling (2nd).

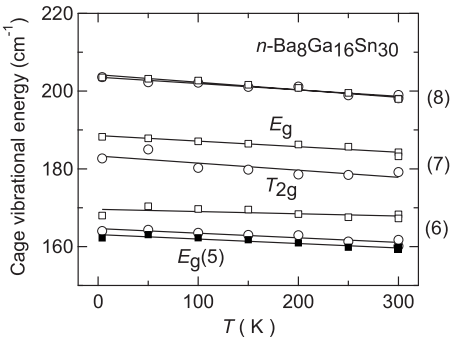

FIG. 5. Temperature dependence of vibrational energy of the cage modes E_g (squares) and T_{2g} (circles) for n-type β-$Ba_8Ga_{16}Sn_{30}$. The closed squares represent $E_g(5)$ (see text).

consequence of the volume contraction upon cooling. By contrast, as is shown in Fig. 6, the energies of the guest $E_g(\mathrm{A})$ and $T_{2g}(1)$ modes decrease by 15% and 25%, respectively. This unusual temperature dependences are explained by considering an anharmonic potential including a quartic term of the temperature-dependent atomic displacement u; $U(u)=k_0+k_2u^2+k_4u^4$. As was discussed for β-EGG and SGG,[15] the guest vibrational energy ω can be described by the equation $\omega^2=\omega_0^2+k_4\langle u^2\rangle$, where ω_0 is the harmonic energy including thermal shrinkage effect. Since the $\langle u^2\rangle$ decreases on cooling, ω^2 and thus the Raman shift decreases with decreasing temperature.

The temperature variations in the energies of $E_g(\mathrm{A})$ and $T_{2g}(1)$ modes for n-type β-BGS are compared with those of β-EGG and SGG in Fig. 6(a). On going from SGG, β-EGG to β-BGS, the rattling energies significantly decrease at room

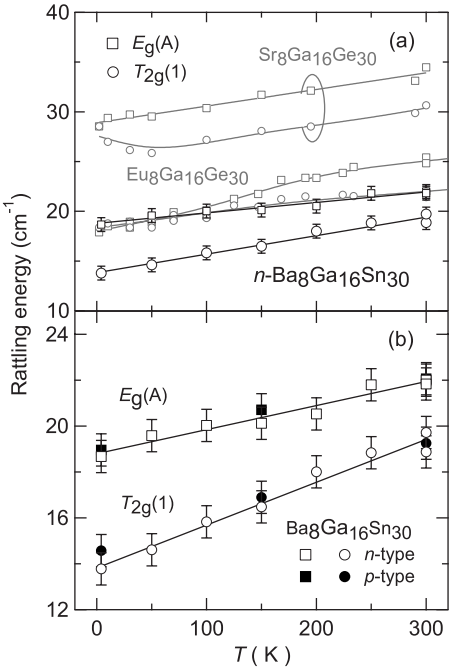

FIG. 6. Temperature dependence of rattling energy of the guest modes $E_g(\mathrm{A})$ and $T_{2g}(1)$ for (a) n-type β-$Ba_8Ga_{16}Sn_{30}$, β-$Eu_8Ga_{16}Ge_{30}$, and $Sr_8Ga_{16}Ge_{30}$ (Refs. 15 and 16), and for (b) n- and p-type β-$Ba_8Ga_{16}Sn_{30}$.

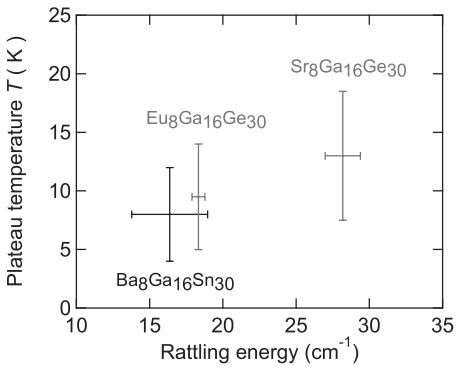

FIG. 7. Temperature range of the plateau in the lattice thermal conductivity $\kappa_L(T)$ versus rattling energy of β-$Ba_8Ga_{16}Sn_{30}$, β-$Eu_8Ga_{16}Ge_{30}$, and $Sr_8Ga_{16}Ge_{30}$. The vertical bars give the temperature range of the plateau shown in Fig. 1 and the horizontal bars are the ranges of rattling energy determined by the Raman-scattering measurements.

temperature. The difference in the energy between $E_g(\mathrm{A})$ and $T_{2g}(1)$ modes increases on cooling for β-BGS while the difference reduces and merges at low temperature for β-EGG and SGG.[15,16] The reason of this difference remains to be studied.

We focus our attention on the fact that the energy of $T_{2g}(1)$ is lower than that of $E_g(\mathrm{A})$. This means that the potential minima are located toward the [100] direction, as was pointed out for SGG.[15,30] This direction points from the high-symmetry 6d site to the off-center 24k sites. At the lowest temperature, the rattling energy of 14 cm^{-1} for β-BGS is lower than those for β-EGG (18 cm^{-1}) and SGG (29 cm^{-1}).[15,16] The energies of β-BGS and SGG agree, respectively, with the values obtained from specific heat analysis using the soft potential model.[8,19] In β-EGG such an analysis is prevented by the strong interference from magnetic degrees of freedom of the Eu^{2+} ions.

Finally, we discuss the relationship between the glasslike $\kappa_L(T)$ and the rattling energy. The temperature ranges of the plateau in $\kappa_L(T)$ for β-BGS, β-EGG, and SGG are indicated by arrows in Fig. 1. In each designated range, the temperature derivative of $\kappa_L(T)$, $d\kappa_L/dT$, has a constant, minimum value for each system. The ranges are estimated to be 4–12 K, 5–14 K, and 7.5–18.5 K for β-BGS, β-EGG, and SGG, respectively. This trend of increasing in the plateau temperature is in accord with the sequence of increasing the rattling energy. Figure 7 shows that the temperature of the plateau is proportional to the rattling energy measured below 10 K for the three systems. This fact further corroborates the argument that the phonon resonant scattering by the off-center rattling gives rise to the glasslike plateau in $\kappa_L(T)$.

In off-center rattling systems, the guest atoms may tunnel the barrier between off-center minima.[31,32] However, quantum tunneling would become dominant over the thermal rattling only at temperatures below about 1 K. For SGG, in fact, the tunneling splitting of Sr modes which form a four level system was estimated to be 0.5 K.[29] In order to investigate the tunneling in β-BGS, we need to extend the lowest temperature limit below 0.3 K for Raman-scattering and thermal conductivity measurements.

IV. CONCLUSIONS

Raman-scattering spectroscopy was used to determine the symmetry and energy of guest rattling in type-I clathrate β-BGS with n- and p-type charge carriers. As in the case of β-EGG and SGG, the presence of additional E_g mode indicates that Ba atoms are also rotating among off-center sites in the tetrakaidecahedron. With decreasing temperature, the rattling energies of E_g(A) and T_{2g}(1) mode strongly decrease. Their anomalous temperature dependences are found irrespective of the charge carrier type and attributed to the quartic term of the anharmonic potential. The rattling energy of 14 cm^{-1} for T_{2g}(1) mode on β-BGS is the lowest among type-I intermetallic clathrates.

The comparison of glasslike temperature dependence of the lattice thermal conductivity $\kappa_L(T)$ for β-BGS, β-EGG, and SGG indicated that the temperature of the $\kappa_L(T)$ plateau is in proportion to the rattling energy. This fact shows that the glasslike plateau of $\kappa_L(T)$ originates to the guest rattling among off-center sites. In order to understand the detailed mechanism of glasslike $\kappa_L(T)$, it is essential to know the phonon dispersions and lifetimes, as was reported for BGG and β-EGG.[13,32] For this purpose, inelastic neutron-scattering experiments at low temperatures are necessary.

ACKNOWLEDGMENTS

We thank C. H. Lee for valuable discussions. This work was financially supported by Grants in Aid for Scientific Research from MEXT of Japan, Grants No. 18204032, No. 19051011, No. 20102004, No. 20102005, No. 09J02772, No. 21540238, and No. 21740527

*Present address: Centro de Ciências Naturais e Humanas, Universidade Federal do ABC, Santo André 09210-170, SP, Brazil.

[1] B. C. Sales, B. C. Chakoumakos, R. Jin, J. R. Thompson, and D. Mandrus, Phys. Rev. B **63**, 245113 (2001).
[2] B. C. Chakoumakos, B. C. Sales, D. Mandrus, and V. Keppens, Acta Crystallogr., Sect. B: Struct. Sci. **55**, 341 (1999).
[3] J. Yamaura, S. Yonezawa, Y. Muraoka, and Z. Hiroi, J. Solid State Chem. **179**, 336 (2006).
[4] S. Paschen, W. Carrillo-Cabrera, A. Bentien, V. H. Tran, M. Baenitz, Yu. Grin, and F. Steglich, Phys. Rev. B **64**, 214404 (2001).
[5] A. Bentien, V. Pacheco, S. Paschen, Yu. Grin, and F. Steglich, Phys. Rev. B **71**, 165206 (2005).
[6] G. S. Nolas, J. L. Cohn, G. A. Slack, and S. B. Schujman, Appl. Phys. Lett. **73**, 178 (1998).
[7] J. L. Cohn, G. S. Nolas, V. Fessatidis, T. H. Metcalf, and G. A. Slack, Phys. Rev. Lett. **82**, 779 (1999).
[8] K. Umeo, M. A. Avila, T. Sakata, K. Suekuni, and T. Takabatake, J. Phys. Soc. Jpn. **74**, 2145 (2005).
[9] S. Sanada, Y. Aoki, H. Aoki, A. Tsuchiya, D. Kikuchi, H. Sugawara, and H. Sato, J. Phys. Soc. Jpn. **74**, 246 (2005).
[10] Z. Hiroi, S. Yonezawa, and Y. Muraoka, J. Phys. Soc. Jpn. **73**, 1651 (2004).
[11] R. C. Zeller and R. O. Pohl, Phys. Rev. B **4**, 2029 (1971).
[12] C. H. Lee, I. Hase, H. Sugawara, H. Yoshizawa, and H. Sato, J. Phys. Soc. Jpn. **75**, 123602 (2006).
[13] M. Christensen, A. B. Abrahamsen, N. B. Christensen, F. Juranyi, N. H. Andersen, K. Lefmann, J. Andreasson, and C. R. H. Bahl, Nat. Mater. **7**, 811 (2008).
[14] G. S. Nolas and C. A. Kendziora, Phys. Rev. B **62**, 7157 (2000).
[15] Y. Takasu, T. Hasegawa, N. Ogita, M. Udagawa, M. A. Avila, K. Suekuni, I. Ishii, T. Suzuki, and T. Takabatake, Phys. Rev. B **74**, 174303 (2006).
[16] Y. Takasu, T. Hasegawa, N. Ogita, M. Udagawa, M. A. Avila, K. Suekuni, and T. Takabatake, Phys. Rev. Lett. **100**, 165503 (2008).
[17] R. P. Hermann, W. Schweika, O. Leupold, R. Rüffer, G. S. Nolas, F. Grandjean, and G. J. Long, Phys. Rev. B **72**, 174301 (2005).
[18] M. A. Avila, K. Suekuni, K. Umeo, H. Fukuoka, S. Yamanaka, and T. Takabatake, Appl. Phys. Lett. **92**, 041901 (2008).
[19] K. Suekuni, M. A. Avila, K. Umeo, H. Fukuoka, S. Yamanaka, T. Nakagawa, and T. Takabatake, Phys. Rev. B **77**, 235119 (2008).
[20] K. Suekuni, T. Tanaka, S. Yamamoto, M. A. Avila, K. Umeo, Y. Takasu, T. Hasegawa, N. Ogita, M. Udagawa, and T. Takabatake, J. Electron. Mater. **38**, 1516 (2009).
[21] X. Gonze, J.-M. Beuken, R. Caracas, F. Detraux, M. Fuchs, G.-M. Rignanese, L. Sindic, M. Verstraete, G. Zerah, F. Jollet, M. Torrent, A. Roy, M. Mikami, P. Ghosez, J.-Y. Raty, and D. C. Allan, Comput. Mater. Sci. **25**, 478 (2002).
[22] The ABINIT code is a common project of the Université Catholique de Louvain, Corning Incorporated and other contributors, http://www.abinit.org
[23] N. Troullier and J. L. Martins, Phys. Rev. B **43**, 1993 (1991).
[24] M. Fuchs and M. Scheffler, Comput. Phys. Commun. **119**, 67 (1999).
[25] J. P. Perdew and Y. Wang, Phys. Rev. B **45**, 13244 (1992).
[26] H. J. Monkhorst and J. D. Pack, Phys. Rev. B **13**, 5188 (1976).
[27] X. Gonze and C. Lee, Phys. Rev. B **55**, 10355 (1997).
[28] X. Gonze, Phys. Rev. B **55**, 10337 (1997).
[29] G. K. H. Madsen and G. Santi, Phys. Rev. B **72**, 220301(R) (2005).
[30] G. S. Nolas, T. J. R. Weakley, J. L. Cohn, and R. Sharma, Phys. Rev. B **61**, 3845 (2000).
[31] I. Zerec, V. Keppens, M. A. McGuire, D. Mandrus, B. C. Sales, and P. Thalmeier, Phys. Rev. Lett. **92**, 185502 (2004).
[32] R. P. Hermann, V. Keppens, P. Bonville, G. S. Nolas, F. Grandjean, G. J. Long, H. M. Christen, B. C. Chakoumakos, B. C. Sales, and D. Mandrus, Phys. Rev. Lett. **97**, 017401 (2006).